Nuclear Mathematical and Computational Sciences: A Century in Review, A Century Anew
Gatlinburg, Tennessee, April 6-11, 2003, on CD-ROM, American Nuclear Society, LaGrange Park, IL (2003)

APPROXIMATE S_N ALBEDO BOUNDARY CONDITIONS FOR TWO NON-MULTIPLYING REGIONS AROUND THE CORE OF NEUTRON FISSION CHAIN REACTING SYSTEMS

Hermes Alves Filho and Ricardo C. Barros
Departamento de Modelagem Computacional
Instituto Politécnico, IPRJ
Universidade do Estado do Rio de Janeiro, UERJ
Caixa Postal 97282
28601-970 Nova Friburgo, RJ, Brazil

ABSTRACT

We discuss in this paper the accuracy of approximate discrete ordinates (S_N) albedo boundary conditions for one-speed eigenvalue problems in X,Y-geometry. The S_N albedo matrix substitutes approximately the two non-multiplying regions, e.g., baffle-reflector system around the multiplying medium, as we neglect the transverse leakage terms within the baffle and reflector regions. We show numerical results to a typical test problem to illustrate the efficiency by analyzing the accuracy of the numerical results versus the CPU time of each run.

Key Words: Neutron Fission Reacting Systems, Neutron Transport Theory, Discrete Ordinates, Albedo Boundary Conditions, Nodal methods

1. INTRODUCTION

Clearly the moderator, reflector and structural materials, e.g., baffle, do not generate power in nuclear reactor cores; therefore we claim we could improve the efficiency of discrete ordinates (S_N) codes for criticality calculations by eliminating the explicit numerical calculations within the non-multiplying regions around the active domain [1]. In Ref. [2] we described the approximate S_N albedo boundary conditions for one non-multiplying region, e.g., reflector around thermal nuclear reactor cores, and discuss the accuracy of the numerical results for a typical model problem. In Ref. [3] we discussed the efficiency of approximate one-region S_N albedo boundary conditions for nuclear reactor global calculations, by analyzing the accuracy of the numerical results for a critical system versus the CPU execution time of each run. The bottom line of the conclusions from this research is that, without losing too much accuracy, the use of approximate S_N albedo boundary conditions for one non-multiplying region reduced significantly the CPU execution time of each run, particularly for fine-grid calculations, e.g., diamond difference (DD) runs.

In this paper we discuss the efficiency of approximate S_N albedo boundary conditions for two non-multiplying regions, e.g., baffle-reflector system around thermal nuclear reactor cores. We

implemented these albedo boundary conditions in a coarse-mesh code, such as the hybrid SD-SGF-CN code [4], and in a fine–mesh code, such as the conventional DD code [5].

In deriving the two region S_N albedo matrix, we transverse-integrate the one-speed S_N equations in X,Y geometry inside the baffle-reflector system contiguous to the active boundary cell of the spatial grid set up on the domain. That is, for the x direction, we integrate the S_N equations inside the baffle-reflector system in the y direction, neglect the transverse leakage terms and solve the resulting homogeneous "one-dimensional" transverse-integrated S_N nodal equations in the x direction analytically by performing a spectral analysis [6]. The procedure follows two major steps: (i) the use of the familiar discretized spatial balance S_N equations [5], with neglect of the leakage terms in the y direction, and (ii) the use of the spectral Green's function (SGF) auxiliary equations, that have parameters to preserve the analytical general solution of the homogeneous "one-dimensional" transverse integrated S_N nodal equations in the x direction. The procedure for the y direction follows similar steps. Therefore, by substituting the SGF auxiliary equations into the discretized spatial balance S_N equations, we can relate the neutron angular fluxes backscattered into the active cell to the neutron angular fluxes entering the baffle from the active cell, since vacuum boundary conditions apply on the outer boundaries of the reflector regions.

We remark that the only approximation that we consider in the derivation of the S_N albedo matrices for S_N eigenvalue problems in X,Y geometry is the neglect of the transverse leakage terms. Therefore, should this approximation introduce no significant errors, we expect the use of the present two-region albedo boundary conditions to improve the efficiency of S_N codes for criticality calculations, in the sense we have described in this section, except for calculations one very coarse spatial grids.

At this point, we present an outline of the remainder of this paper. In section 2, we describe how we determine the approximate S_N two-region albedo matrices. In section 3, we show numerical results to a typical model problem, and in section 4 we list a number of concluding remarks and suggestions for future work.

2. APPROXIMATE S_N ALBEDO FOR TWO NON-MULTIPLYING REGIONS

Let us consider a rectangular spatial grid Ω, where each cell $\Omega_{i,j}$ has width h_i and height k_j, with i = 1 : I and j = 1 : J. Viz Figure 1. Now, we consider the one-speed S_N equations in X,Y geometry with isotropic scattering

$$\mu_m \frac{\partial}{\partial x} \psi_m(x,y) + \eta_m \frac{\partial}{\partial y} \psi_m(x,y) + \sigma_T \psi_m(x,y) = \sigma_S \sum_{n=1}^{M} \psi_n(x,y)\, w_n, \qquad (1)$$
$$m = 1 : M, \qquad M = N(N+2)/4 \ .$$

Here the notation is standard [5] and Eq. (1) holds inside a homogeneous non-multiplying medium, e.g., baffle and reflector regions around thermal nuclear reactor cores for example. By

integrating Eq.(1) inside the baffle cf. Figure 1, we obtain the familiar discretized spatial balance S_N equations

$$\frac{\mu_m}{L_b}\left[\tilde{\psi}_{m,j}(x_b)-\tilde{\psi}_{m,j}(x_a)\right]+\frac{\eta_m}{k_j}\left[\hat{\psi}_{m,b}(y_{j+1/2})-\hat{\psi}_{m,b}(y_{j-1/2})\right]+$$
$$\sigma_{T_b}\overline{\psi}_{m,b,j}=\sigma_{S_b}\sum_{n=1}^{M}\overline{\psi}_{n,b,j}w_n \quad , m=1:M \quad , \tag{2}$$

where we have used the following definitions:

$\tilde{\psi}_{m,j}(x)$ = y-direction node-edge average angular flux.

$\hat{\psi}_{m,b}(y)$ = x-direction node-edge average angular flux in the baffle.

$\overline{\psi}_{m,b,j}$ = node-average angular flux in the baffle region of height k_j, cf. Figure 1.

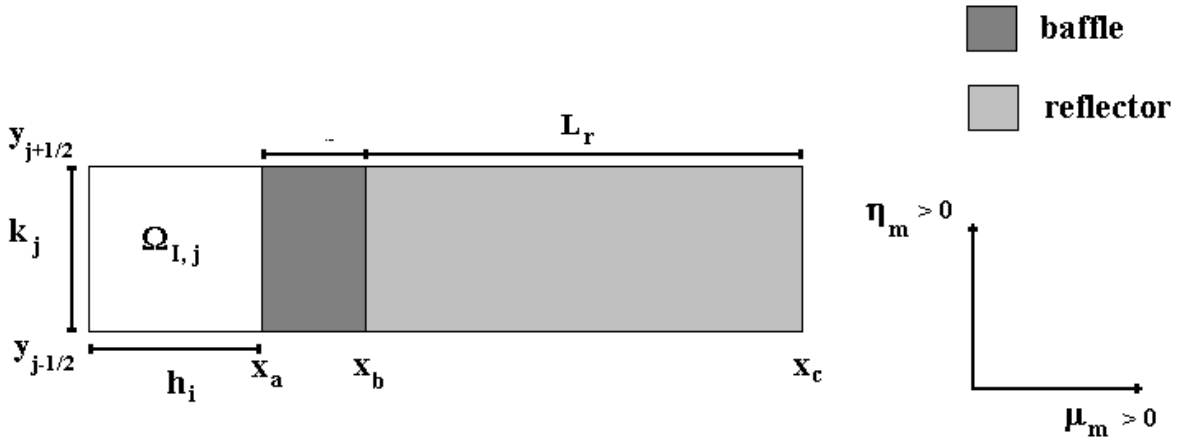

Figure 1. Albedo for two non-multiplying regions.

Following similar steps for the reflector, we integrate Eq. (1) inside the reflector region and we obtain

$$\frac{\mu_m}{L_r}\left[\tilde{\psi}_{m,j}(x_c)-\tilde{\psi}_{m,j}(x_b)\right]+\frac{\eta_m}{k_j}\left[\hat{\psi}_{m,r}(y_{j+1/2})-\hat{\psi}_{m,r}(y_{j-1/2})\right]+$$
$$\sigma_{T_r}\overline{\psi}_{m,r,j}=\sigma_{S_r}\sum_{n=1}^{M}\overline{\psi}_{n,r,j}w_n \quad , m=1:M \quad , \tag{3}$$

where $\hat{\psi}_{m,r}(y)$ is the x-direction node-edge average angular flux in the reflector, and $\overline{\psi}_{m,r,j}$ is the average angular flux in the reflector region of height k_j, cf. Figure 1.

In order to determine the approximate S_N albedo for the x direction, we neglect the transverse leakage terms in the y direction in Eqs. (2) and (3) to obtain the "one-dimensional" discretized spatial balance S_N equations

$$\frac{\mu_m}{L_b}\left[\tilde{\psi}_{m,j}(x_b)-\tilde{\psi}_{m,j}(x_a)\right]+\sigma_{T_b}\,\overline{\psi}_{m,b,j}=\sigma_{S_b}\sum_{n=1}^{M}\overline{\psi}_{n,b,j}w_n\ ,\ m=1:M\quad , \tag{4}$$

$$\frac{\mu_m}{L_r}\left[\tilde{\psi}_{m,j}(x_c)-\tilde{\psi}_{m,j}(x_b)\right]+\sigma_{T_r}\,\overline{\psi}_{m,r,j}=\sigma_{S_r}\sum_{n=1}^{M}\overline{\psi}_{n,r,j}w_n\ ,\ m=1:M\quad . \tag{5}$$

Furthermore we consider the SGF auxiliary equations

$$\overline{\psi}_{m,b,j}=\sum_{\mu_n>0}\theta^{b}_{m,n}\,\tilde{\psi}_{n,j}(x_a)+\sum_{\mu_n<0}\theta^{b}_{m,n}\,\tilde{\psi}_{n,j}(x_b)\ ,\qquad m=1:M\ , \tag{6}$$

and

$$\overline{\psi}_{m,r,j}=\sum_{\mu_n>0}\theta^{r}_{m,n}\,\tilde{\psi}_{n,j}(x_b)+\sum_{\mu_n<0}\theta^{r}_{m,n}\,\tilde{\psi}_{n,j}(x_c)\ ,\qquad m=1:M\ , \tag{7}$$

where the parameters $\theta^{b/r}_{m,n}$ relate the node-average angular flux within the baffle/reflector in a fixed angular direction *m* to the node-edge average angular fluxes in all the incoming directions. To determine the parameters $\theta^{b/r}_{m,n}$ we first find the expression for the local general solution of the transverse integrated S_N nodal equations in the x direction with neglect of the transverse leakage terms within the baffle/reflector, and then, we substitute it into the SGF auxiliary equations (6) or (7) accordingly bearing in mind the average definitions. A detailed description of this procedure can be found in Ref. [7].

Further, we substitute the SGF auxiliary equations (6) into Eq. (4) and then, considering that vacuum boundary conditions usually apply on the outer boundaries of the reflector regions for criticality calculations, we simplify the SGF auxiliary equations (7) and substitute them into Eq. (5). Therefore, we are left with a system of 3M/2 algebraic linear equations in 2M unknowns that are the y-direction node-edge average angular fluxes.

After some algebra, we can relate the y-direction node-edge average angular fluxes backscattered into the fuel node $\Omega_{I,j}$ to the angular fluxes entering the baffle at $x=x_a$, that is

$$\tilde{\boldsymbol{\Psi}}_j^{\mu_m < 0}(x_a) = \underline{\underline{\Lambda}}_x^R \tilde{\boldsymbol{\Psi}}_j^{\mu_m > 0}(x_a) \quad , \tag{8}$$

where we have defined

$\underline{\underline{\Lambda}}_x^R$ = two-region approximate S_N albedo matrix to the right-hand side boundary of the domain, viz Figure 1.

$\tilde{\boldsymbol{\Psi}}_j^{\mu_m \lessgtr 0}(x_a)$ = M/2 – dimensional vector whose components are the y–direction node–edge average angular fluxes at $x = x_a$ entering the baffle region ($\mu_m > 0$) or entering the fuel region ($\mu_m < 0$).

To obtain the two-region albedo matrices for the left-hand side boundary conditions, as well as for the top and bottom, we proceed similarly.

3. NUMERICAL RESULTS

In this section we show numerical results to a test problem that we model using the level symmetric S_4 angular quadrature set [5]. This model problem consists of a heterogeneous critical system, composed of four different material zones, viz Figure 2, whose material data are listed in Table I [8].

Table II displays the numerical results generated for the effective multiplication factor (k_{eff}) by the hybrid SD-SGF-CN method [4] on various spatial grids with (i) explicit baffle-reflector system; (ii) explicit baffle and albedo for the reflector (SD-SGF-CN_{alb1R}); and (iii) two-region albedo boundary conditions (SD-SGF-CN_{alb2R}). As we see, the use of albedo boundary conditions does not increase significantly the relative deviations with respect to the fine-grid results generated by the conventional DD method with explicit baffle-reflector system. In addition, the CPU execution time for the albedo calculations also decreased with respect to the explicit baffle-reflector system calculations. Based on the results that we show in Table II for this critical model problem, we conclude that without increasing too much the relative deviations of the numerical results generated by the SD-SGF-CN method for the eigenvalue k_{eff} with respect to the reference DD result, the one-region albedo calculations reduced the execution time by 27 % for the Γ_3 run up to 47 % for the Γ_7 run. On the other hand, the two region albedo calculations reduced the execution time by 31 % for the Γ_3 run up to 74 % for the Γ_7 run. This means a gain in efficiency in the sense we have described in section 1, On the other hand, the two region albedo calculations reduced the execution time by 31 % for the Γ_3 run up to 74 % for the Γ_7 run. This means a gain in efficiency in the sense we have described in section 1, and we emphasize that the CPU execution time of each run included the calculation of the albedo matrix entries. Moreover, Table II also lists the results generated for the eigenvalue k_{eff} by the fine-mesh DD method (Γ_8 run) with one- and two-region albedo boundary conditions. We note that the use of one-region albedo boundary conditions reduced the execution time by 64 %, whereas

the use of two-region albedo boundary conditions reduced the execution time by 83 % for the Γ_8 DD runs. We remark that the albedo DD runs generated relative deviations, which are comparable to the ones generated by SD-SGF-CN method with albedo boundary conditions on a spatial grid composed of 16 nodes per region in each spatial direction (Γ_6 run, 141.7 seconds and 72.55 seconds).

Supposing that the power density generated by the entire domain is 1 Watt/cm^3, Figure 3 shows the power density distribution as generated by six independent runs with explicit two non-multiplying region calculations, one–region albedo and two-region albedo calculations, using both the coarse-mesh SD-SGF-CN method on the Γ_4 spatial grid, and the fine-mesh DD method on the Γ_8 spatial grid. As we see in Figure 4, although the relative deviations for this numerical experiment are still acceptable for practical applications, we remark that the two-region albedo calculations, generate less accurate results for the boundary regions, mainly for the corner regions, that have two sides interfacing the baffle-moderator system. This is probably due to the fact the boundary regions are more sensitive to the effects of the approximations involved in the present albedo boundary conditions than the interior regions. We remark that this is specially evident for the corner regions with two sides on the baffle-moderator boundary.

Table I. Material Data.

Zone Number	σ_T (cm^{-1})	σ_S (cm^{-1})	$\nu\sigma_F$ (cm^{-1})
1 (Pu – 239)	3.26400E-1[a]	2.25216E-1	0.11491E+0
2 (Pu - 239)	3.26400E-1	2.25216E-1	0.10072E+0
3 (baffle)	3.30600E-2	7.39000E-3	0.0
4 (reflector)	3.26400E-1	2.93760E-1	0.0

[a] Read as 3.26400 x 10^{-1}.

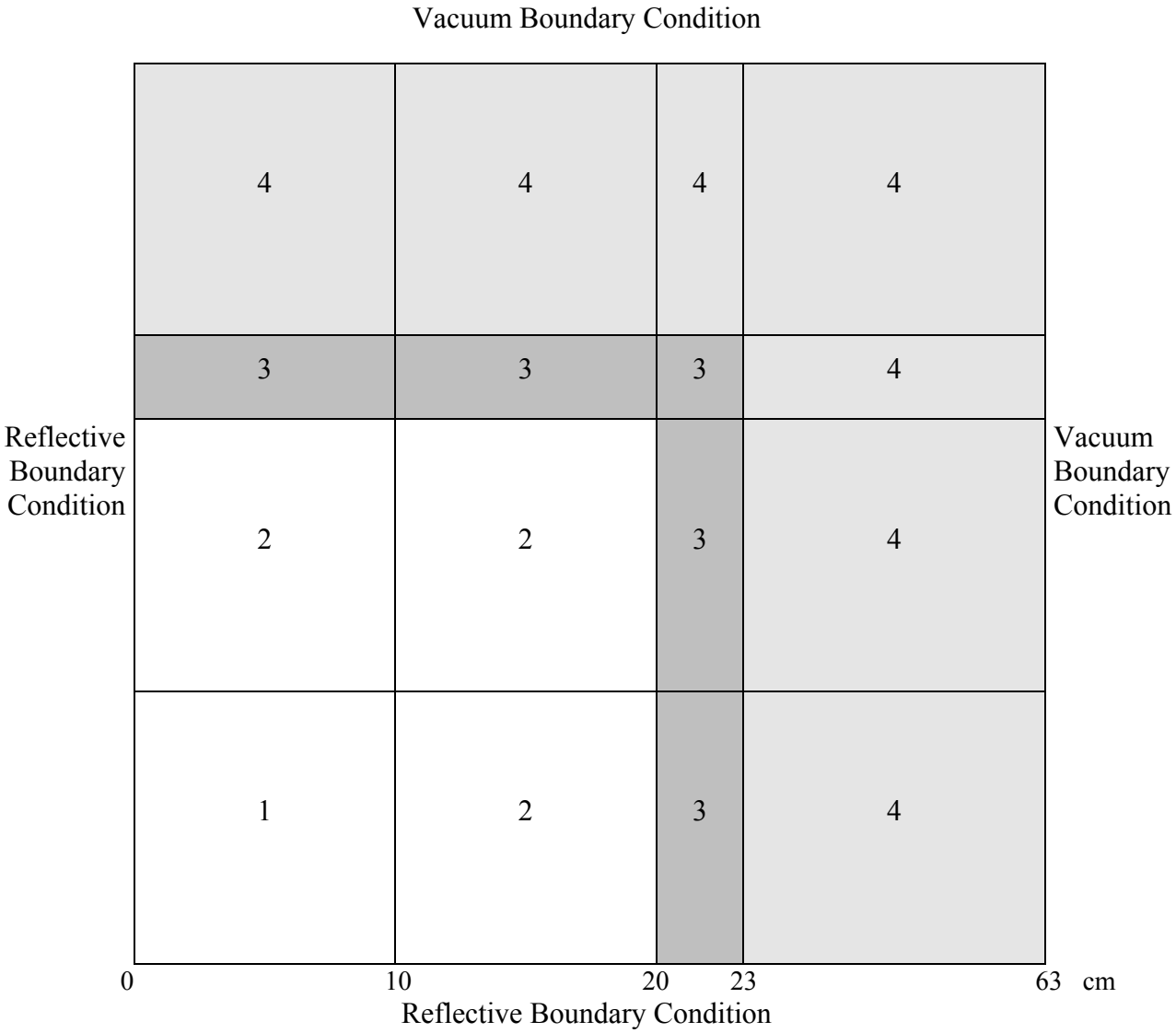

Figure 2. Model Problem.

Table II. Numerical Results for the Model Problem.

Spatial Grid Γ_n [a]	Numerical Method	Dominant Eigenvalue (k_{eff})	Relative Deviation (%) [h]	CPU time [i] (seconds)	CPU time reduction (%)
Γ_3	SD-SGF-CN [b]	0.99698	0.15	14.870	
	$SD\text{-}SGF\text{-}CN_{alb1R}$ [c]	0.99719	0.17	10.810	27
	$SD\text{-}SGF\text{-}CN_{alb2R}$ [d]	1.00179	0.63	10.230	31
Γ_4	SD-SGF-CN	0.99598	0.05	24.640	
	$SD\text{-}SGF\text{-}CN_{alb1R}$	0.99631	0.08	17.800	28
	$SD\text{-}SGF\text{-}CN_{alb2R}$	1.00111	0.56	14.230	42
Γ_5	SD-SGF-CN	0.99564	0.01	69.660	
	$SD\text{-}SGF\text{-}CN_{alb1R}$	0.99606	0.06	42.990	38
	$SD\text{-}SGF\text{-}CN_{alb2R}$	1.00084	0.54	25.820	63
Γ_6	SD-SGF-CN	0.99554	0.0	249.020	
	$SD\text{-}SGF\text{-}CN_{alb1R}$	0.99599	0.05	141.700	43
	$SD\text{-}SGF\text{-}CN_{alb2R}$	1.00079	0.53	72.550	71
Γ_7	SD-SGF-CN	0.99552	0.0	988.740	
	$SD\text{-}SGF\text{-}CN_{alb1R}$	0.99598	0.05	536.210	47
	$SD\text{-}SGF\text{-}CN_{alb2R}$	1.00077	0.53	257.790	74
Γ_8	DD-CBI [e]	0.99549		5654.720	
	DD_{alb1R} [f]	0.99560	0.05	2062.860	64
	DD_{alb2R} [g]	1.00075	0.53	946.870	83

[a] $2^n / 4$ spatial nodes per region in each spatial direction.

[b] *Spectral diamond-spectral Green's function-constant nodal* method with explicit reflector and baffle.

[c] *Spectral diamond-spectral Green's function-constant nodal* method with albedo boundary conditions for one non-multiplying region.

[d] *Spectral diamond-spectral Green's function-constant nodal* method with albedo boundary conditions for two non-multiplying regions.

[e] *Diamond difference* method with explicit reflector and baffle (reference result).

[f] *Diamond difference* method with albedo boundary conditions for one non-multiplying region.

[g] *Diamond difference* method with albedo boundary conditions for two non-multiplying regions.

[h] Relative deviation with respect to the DD fine-mesh solution.

[i] On a Pentium III 850-MHz PC

******4.9920E-2 *****4.8550E-2 ****4.8423E-2 ***4.8494E-2 **4.8675E-2 *5.0040E-2	******2.7150E-2 *****2.5190E-2 ****2.5138E-2 ***2.5122E-2 **2.5167E-2 *2.7130 E-2		
******0.1230E+0 *****0.1277E+0 ****0.1280E+0 ***0.1279E+0 **0.1275E+0 *0.1228E+0	******4.9920E-2 *****4.8550E-2 ****4.8423E-2 ***4.8494E-2 **4.8675E-2 *5.0040E-2		

Figure 3. Power Density Distribution.

****** SD-SGF-CN results with albedo boundary conditions for two non-multiplying regions and Γ_4 spatial grid.

***** SD-SGF-CN results with albedo boundary conditions for one non-multiplying region and Γ_4 spatial grid.

**** SD-SGF-CN results with explicit reflector and baffle and Γ_4 spatial grid.

*** *Diamond difference* results with explicit reflector and baffle and Γ_8 spatial grid

** *Diamond difference* results with albedo boundary conditions for one non-multiplying regions and Γ_8 spatial grid.

* *Diamond difference* results with albedo boundary conditions for two non-multiplying regions and Γ_8 spatial grid.

*****2.93 ****0.11 ***0.15 **0.37 *3.18	*****8.08 ****0.26 ***0.06 **0.18 *7.99		
*****3.81 ****0.13 ***0.09 **0.0 *3.98	*****2.93 ****0.11 ***0.15 **0.37 *3.18		

Figure 4. Relative Deviation (%) for the Power Density Distribution

***** SD-SGF-CN results with albedo boundary conditions for two non-multiplying regions and Γ_4 spatial grid.

**** SD-SGF-CN results with albedo boundary conditions for one non-multiplying region and Γ_4 spatial grid.

*** SD_SGF-CN results with explicit reflector and baffle and Γ_4 spatial grid

** *Diamond difference* results with albedo boundary conditions for one non-multiplying regions and Γ_8 spatial grid.

* *Diamond difference* results with albedo boundary conditions for two non-multiplying regions and Γ_8 spatial grid.

4. CONCLUDING REMARKS

Based on the numerical experiments described in the previous section, we list a number of general conclusions and suggestions for future work:

- the approximate one- and two-region S_N albedo boundary conditions for criticality calculations substitute accurately the non-multiplying regions around the active core;

- without losing too much accuracy, the use of albedo boundary conditions reduced significantly the CPU execution time of each run. This is particularly noticeable for fine-grid calculations;

- the S_N albedo boundary conditions, as described in this paper, can be implemented in various conventional numerical methods for one-speed X,Y–geometry S_N criticality calculations, such as the DD method, the step-characteristic method and the discontinuous finite element methods;

- criticality calculations with two-region S_N albedo boundary conditions generate less accurate results for the boundary regions, mainly for the corner regions. We remark that this is problem dependent, and we expect that numerical results for more localized quantities will be more sensitive to the approximations involved in the present two-region S_N albedo boundary conditions than for global quantities, mainly for the corner regions.

- for practical applications in nuclear reactor global calculations we are now working on the multigroup approximate S_N albedo boundary conditions that are of great interest to account for the neutron energy change in nuclear interactions. We intend to report on the numerical results when they are fully tested.

ACKNOWLEDGMENTS

This work was sponsored by CNPq and UERJ – Brazil.

REFERENCES

1. S. Rauck and R. Sanchez, “Multigroup Albedo Method”, *Proceedings of the International Conference on Mathematics and Computation, Reactor Physics and Environmental Analyses,* Madrid, Spain, September 09-13, Vol. 2, pp. 891-900 (1999).

2. H. Alves Filho and R. C. Barros, “Discrete Ordinates Albedo Boundary Conditions for One-Speed Eigenvalue Problems in X, Y Geometry”, *Proceedings of the 2001 International Meeting on Mathematical Methods for Nuclear Applications*, Salt Lake City, Utah, USA September 09-13, CD-ROM (2001).

3. H. Alves Filho and R. C. Barros, "On the Efficiency of Approximate S_N Albedo Boundary Conditions for Monoenergetic X, Y-Geometry Criticality Calculations", Multigroup Albedo Method", *Proceedings of the International Conference on Mathematics and Computation, Reactor Physics and Environmental Analyses,* Seoul, Korea, October 7-10, Vol. 1, pp. 1-9 (2002).

4. H. Alves Filho, R.C. Barros and F.C. da Silva, "The Hybrid Spectral Diamond-Spectral Green's Function-Constant Nodal Method for One-Speed X,Y-Geometry S_N Eigenvalue Problems", *Proceedings of the International Conference on Mathematics and Computation, Reactor Physics and Environmental Analyses*, Madrid, Spain, September 09-13, Vol. 2, , pp. 1608-1617 (1999).

5. E.E. Lewis and W.F. Miller Jr, *Computational Methods of Neutron Transport*, American Nuclear Society, La Grange Park, Illinois, USA (1984).

6. R.C. Barros, H. Alves Filho and F.C. da Silva, "Recent Advances in Spectral Nodal Methods for X,Y-Geometry Discrete Ordinates Deep Penetration and Eigenvalue Problems", *Progress in Nuclear Energy*, **35**, pp. 293-331 (1999).

7. R.C. Barros and E.W. Larsen, "A Spectral Nodal Method for One-Group X, Y-Geometry Discrete Ordinates Problems", *Nuclear Science and Engineering*, **111**, pp. 34-45 (1992).

8. A. Sood, R. A. Forster and D. K. Parsons, "Analytical Benchmark Test Set for Criticality Code Verification", LA-13511 (1999).